

This document contains a post-print version of the paper

Deflection Model of A Multi-Actuator Gap Leveler

authored by **R. Brauneis, M. Baumgart, A. Steinboeck, A. Kugi, and M. Jochum**

and published in *IFAC-PapersOnLine*.

The content of this post-print version is identical to the published paper but without the publisher's final layout or copy editing. Please, scroll down for the article.

Cite this article as:

R. Brauneis, M. Baumgart, A. Steinboeck, A. Kugi, and M. Jochum, "Deflection model of a multi-actuator gap leveler", *IFAC-PapersOnLine*, vol. 50, no. 1, pp. 11 295–11 300, 2017, ISSN: 2405-8963. DOI: [10.1016/j.ifacol.2017.08.1647](https://doi.org/10.1016/j.ifacol.2017.08.1647)

BibTex entry:

```
@Article{BRAUNEIS201711295,  
  author = {R. Brauneis and M. Baumgart and A. Steinboeck and A. Kugi and M. Jochum},  
  title = {Deflection Model of A Multi-Actuator Gap Leveler},  
  journal = {IFAC-PapersOnLine},  
  year = {2017},  
  volume = {50},  
  number = {1},  
  pages = {11295--11300},  
  issn = {2405-8963},  
  doi = {10.1016/j.ifacol.2017.08.1647},  
  keywords = {Optimal control, feedforward control, steel industry, deflection compensation, cold leveling,  
    leveler for heavy plates, analytical leveling model},  
  owner = {rbr},  
  timestamp = {2017.10.23},  
  url = {http://www.sciencedirect.com/science/article/pii/S2405896317322504},  
}
```

Link to original paper:

<http://dx.doi.org/10.1016/j.ifacol.2017.08.1647>
<http://www.sciencedirect.com/science/article/pii/S2405896317322504>

Read more ACIN papers or get this document:

<http://www.acin.tuwien.ac.at/literature>

Contact:

Automation and Control Institute (ACIN)
TU Wien
Gusshausstrasse 27-29/E376
1040 Vienna, Austria

Internet: www.acin.tuwien.ac.at
E-mail: office@acin.tuwien.ac.at
Phone: +43 1 58801 37601
Fax: +43 1 58801 37699

Copyright notice:

This is the authors' version of a work that was accepted for publication in *IFAC-PapersOnLine*. Changes resulting from the publishing process, such as peer review, editing, corrections, structural formatting, and other quality control mechanisms may not be reflected in this document. Changes may have been made to this work since it was submitted for publication. A definitive version was subsequently published in R. Brauneis, M. Baumgart, A. Steinboeck, A. Kugi, and M. Jochum, "Deflection model of a multi-actuator gap leveler", *IFAC-PapersOnLine*, vol. 50, no. 1, pp. 11 295–11 300, 2017, ISSN: 2405-8963. DOI: [10.1016/j.ifacol.2017.08.1647](https://doi.org/10.1016/j.ifacol.2017.08.1647)

Deflection Model Of A Multi-Actuator Gap Leveler

R. Brauneis* M. Baumgart* A. Steinboeck* A. Kugi*
M. Jochum**

* Automation and Control Institute, Technische Universität Wien,
1040 Vienna, Austria (e-mail:brauneis@acin.tuwien.ac.at)

** AG der Dillinger Hüttenwerke, 66763 Dillingen, Germany

Abstract: In this paper, a mathematical deflection model of a leveler for cold heavy plates is presented. The model calculates the work roll profile and the leveling forces for a given plate and adjustment of the leveler. The force-deflection relations of the machine model are combined with a nonlinear plate model and solved for the unknown displacements of the work rolls. The plate model is based on a leveling model found in literature. The analytical solution of this model ensures a short computation time. Therefore, the model is suitable for feedforward control and optimization. Finally, the model serves as a basis for calculating the optimal adjustment of the leveler subject to force constraints, which avoids overloading of the machine.

Keywords: Optimal control, feedforward control, steel industry, deflection compensation, cold leveling, leveler for heavy plates, analytical leveling model

1. INTRODUCTION

Leveling is a production step in rolling mills to reduce flatness defects and residual stresses of plates after rolling. As a final production step, cold levelers are used to ensure a flat product and to establish a desired residual stress distribution in the plate. This process is critical for the product quality because it is the last deformation step before leaving the rolling mill. During the leveling process, the work rolls of the leveler (c.f. Fig. 1) impose a sequence of carefully planned, alternate bending steps onto the plate, which passes through the leveler. The vertical adjustment of the work rolls determines the local curvature of the plate, and therefore its plastification rate. The forces occurring during the leveling process are in the range of several meganewtons and cause significant deformation of the machine. This is why the work rolls may deviate from their nominal positions, which can result in a lower plastification rate than required. Thus, the deflection has to be compensated. High leveling forces may also lead to local overloading of the support rolls, which must be avoided.

To ensure consistent product quality and throughput while also maintaining safe operating conditions the leveling process has to be automatized. Because neither the deflection nor the internal forces of the leveler can be measured, an accurate force/deflection model is required. The leveling process itself has been studied extensively in the literature. Henrich (1993), Doege et al. (2002) and Menz (2002) developed semi-analytical models of the leveling process. Batty and Lawson (1965) presented force and power requirements of the leveling process based on the analytical solution of the consecutive bending process. Modern approaches as in (Liu et al., 2012) are either based on the finite element method or incorporate another tailored numerical model. However, the described works

do not incorporate the deflection of the work rolls and the machine. Mischke and Jonca (1992) implemented a rudimentary deflection model of the work rolls. Krämer et al. (2011) and Bodini et al. (2007) presented successful implementations of fully automatized leveling processes. Baumgart et al. (2011, 2012, 2015) developed a detailed deflection model by combining a machine model and a simple plate model. Furthermore, an optimal controller of the adjustment of a hot leveler was presented.

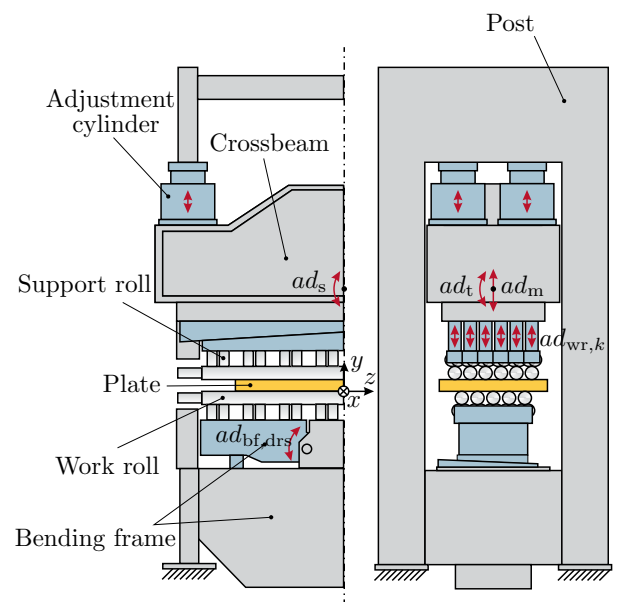


Fig. 1. Front and side view of the leveler.

As shown in Fig. 1, the considered leveler has 11 work rolls, where the 6 upper work rolls can be individually adjusted. It operates at a rolling mill of AG der Dillinger Hüttenwerke. The upper rolls are held in place by a crossbeam, which can be vertically moved and slightly tilted via four adjustment cylinders. To compensate for the bending deflection of the machine and to treat non-developable flatness defects of the plate, the lower part of the leveler features a bending frame, which can pre-bend the lower work rolls. In total, the machine offers 11 degrees of freedom (adjustment variables) to control the roll intermesh.

In this paper, a mathematical model of the deformation of the machine for given adjustment values and plate properties is presented. The proposed approach features an efficient implementation and low computational costs. Furthermore, the developed model serves as a basis for determining adjustment settings which achieve an optimal compensation of the deflection with respect to the leveling quality while respecting the maximum feasible support roll forces. The paper is organized as follows: In the first two sections the machine and the plate model will be derived. The combination of both models, which yields the full deflection model, will be presented in the third section. Finally, the feasibility of this approach is shown in the last section, where an example of the application to determine optimal adjustment values is given.

2. MACHINE MODEL

In this section, the deflection model of the machine is derived. Some parts of this model are adopted from (Baumgart et al., 2011). The main purpose of the machine model is to calculate the shape and position of the work rolls for a given distributed load $q_k(z)$ on each work roll k . Additionally, the contact forces between the work and support rolls are determined.

The machine consists of several elastic components which contribute to the deflection. The crossbeam, the adjustment cartridge with the (upper) support rolls and the posts belong to the upper frame. The lower frame consists of the bending frame with the lower support rolls and the lower crossbeam. The 11 degrees of freedom can be grouped into vectors according to their influence on the adjustment of the leveler. The vector $\mathbf{ad}_{\text{wr}} = [ad_{\text{wr},k}]^T$ with $k \in \{1, 3, 5, 7, 9, 11\}$ contains the 6 individual adjustments of the upper work rolls, the vector $\mathbf{ad}_{\text{tr}} = [ad_m, ad_t, ad_s]^T$ the 3 degrees of freedom of the upper crossbeam, and the vector $\mathbf{ad}_{\text{bf}} = [ad_{\text{bf,drs}}, ad_{\text{bf,ops}}]^T$ the 2 tilting angles of the bending frames.

Similar to (Baumgart et al., 2011), the work rolls are modeled as Euler-Bernoulli beams. To solve the static beam equation with multiple complex boundary conditions, a finite element model of the work rolls is used. The rolls are discretized along the axis z with the mesh \mathbf{z}_{wr} . A subset $\tilde{\mathbf{z}}_{\text{wr}}$ of these nodes coincides with the support roll nodes \mathbf{z}_{sr} and the relation $\mathbf{z}_{\text{sr}} = \tilde{\mathbf{z}}_{\text{wr}} = \tilde{\mathbf{U}}\mathbf{z}_{\text{wr}}$ with an appropriate mapping Matrix $\tilde{\mathbf{U}}$ can be formulated. The center points of the rolls along the axis x are assembled in the vector \mathbf{x}_{wr} .

Assuming that the rotational displacements of the upper crossbeam are small, their influence on the x and z coordinates of the nodes is negligible. The rigid body positions y of the nodes can then be expressed in terms of the adjustment $\mathbf{ad} = [\mathbf{ad}_{\text{tr}}^T, \mathbf{ad}_{\text{wr}}^T, \mathbf{ad}_{\text{bf}}^T]^T$ in the form

$$\mathbf{y}_{\text{wr},0} = \begin{bmatrix} \mathbf{y}_{\text{wr},0}^{\text{up}}(\mathbf{ad}_{\text{wr}}, \mathbf{ad}_{\text{tr}}) \\ \mathbf{y}_{\text{wr},0}^{\text{lo}} \end{bmatrix} \quad (1)$$

for the work rolls and

$$\mathbf{y}_{\text{sr},0} = \begin{bmatrix} \mathbf{y}_{\text{sr},0}^{\text{up}}(\mathbf{ad}_{\text{wr}}, \mathbf{ad}_{\text{tr}}) \\ \mathbf{y}_{\text{sr},0}^{\text{lo}}(\mathbf{ad}_{\text{bf}}) \end{bmatrix} \quad (2)$$

for the support rolls. The nodes of the upper and lower frame are labeled with the superscript up and lo , respectively.

The linear force-deflection relations of the work rolls can be defined by block-diagonal stiffness matrices $\mathbf{K}_{\text{wr}}^{\text{up}}$ and $\mathbf{K}_{\text{wr}}^{\text{lo}}$ for all upper and lower work rolls. The upper and the lower frames of the machine consist of several complex parts. The force-deflection relations of these structures are derived by finite element models and model reduction techniques. As a result, the stiffness matrices of the upper and the lower frames, $\mathbf{K}_{\text{frm}}^{\text{up}}$ and $\mathbf{K}_{\text{frm}}^{\text{lo}}$, are obtained. With the given nodal forces $\mathbf{F}_{\text{wr}} = [\mathbf{F}_{\text{wr}}^{\text{up}} \ \mathbf{F}_{\text{wr}}^{\text{lo}}]^T$ acting on the work rolls, it is possible to calculate the deflection of the work and support roll nodes. The equilibrium of forces

$$\mathbf{F}_{\text{wr}}^p - \tilde{\mathbf{U}}_p^T \mathbf{F}_{\text{sr}}^p = \mathbf{K}_{\text{wr}}^p \mathbf{u}_{\text{wr}}^p \quad (3a)$$

$$\mathbf{F}_{\text{sr}}^p = \mathbf{K}_{\text{frm}}^p \mathbf{u}_{\text{sr}}^p \quad (3b)$$

can be solved for the deflections \mathbf{u}_{sr}^p and \mathbf{u}_{wr}^p of each frame $p \in \{\text{up}, \text{lo}\}$. To avoid the solution of the nonlinear contact problem between the work and the support rolls, it is assumed that all rolls are in contact when the leveler is loaded. Due to the adjustment of the bending frame, the required relative displacements $\mathbf{u}_{\text{gap}}^{\text{lo}} = \tilde{\mathbf{U}}_{\text{lo}} \mathbf{y}_{\text{wr},0}^{\text{lo}} - \mathbf{y}_{\text{sr},0}^{\text{lo}}(\mathbf{ad}_{\text{bf}})$ to close the gap between the rolls of the lower frame has to be considered. The displacements of the support roll nodes thus read as $\mathbf{u}_{\text{sr}}^{\text{lo}} = \tilde{\mathbf{U}}_{\text{lo}} \mathbf{u}_{\text{wr}}^{\text{lo}} - \mathbf{u}_{\text{gap}}^{\text{lo}}$ and $\mathbf{u}_{\text{sr}}^{\text{up}} = \tilde{\mathbf{U}}_{\text{up}} \mathbf{u}_{\text{wr}}^{\text{up}}$. Using these displacements in (3) yields the effective force-deflection relations

$$\mathbf{u}_{\text{wr}}^{\text{up}} = \left(\mathbf{K}_{\text{wr}}^{\text{up}} + \tilde{\mathbf{K}}_{\text{frm}}^{\text{up}} \right)^{-1} \mathbf{F}_{\text{wr}}^{\text{up}} \quad (4a)$$

$$\mathbf{u}_{\text{wr}}^{\text{lo}} = \left(\mathbf{K}_{\text{wr}}^{\text{lo}} + \tilde{\mathbf{K}}_{\text{frm}}^{\text{lo}} \right)^{-1} \left(\mathbf{F}_{\text{wr}}^{\text{lo}} + \tilde{\mathbf{U}}_{\text{lo}}^T \mathbf{K}_{\text{frm}}^{\text{lo}} \mathbf{u}_{\text{gap}}^{\text{lo}} \right) \quad (4b)$$

with $\tilde{\mathbf{K}}_{\text{frm}}^p = \tilde{\mathbf{U}}_p^T \mathbf{K}_{\text{frm}}^p \tilde{\mathbf{U}}_p$. The absolute positions of the work roll nodes

$$\mathbf{y}_{\text{wr}}^{\text{up}} = \mathbf{y}_{\text{wr},0}^{\text{up}}(\mathbf{ad}_{\text{wr}}, \mathbf{ad}_{\text{tr}}) + \mathbf{u}_{\text{wr}}^{\text{up}}(\mathbf{F}_{\text{wr}}^{\text{up}}) \quad (5a)$$

$$\mathbf{y}_{\text{wr}}^{\text{lo}} = \mathbf{y}_{\text{wr},0}^{\text{lo}} + \mathbf{u}_{\text{wr}}^{\text{lo}}(\mathbf{ad}_{\text{bf}}, \mathbf{F}_{\text{wr}}^{\text{lo}}) \quad (5b)$$

are then obtained by adding the deflections \mathbf{u}_{wr}^p to the undeformed nodal positions $\mathbf{y}_{\text{wr},0}^p$. This yields the final machine model

$$\mathbf{y}_{\text{wr}} = [\mathbf{y}_{\text{wr}}^{\text{up}} \ \mathbf{y}_{\text{wr}}^{\text{lo}}]^T = \mathbf{f}(\mathbf{ad}, \mathbf{F}_{\text{wr}}) \quad (6)$$

for the work roll profiles.

The machine model (6) was verified by loading the leveler with five independent test beams and measuring the change of the roll intermesh $\Delta \mathbf{y}_{\text{im, meas}, k}$ (c.f. Fig. 2) while rising the force in all four adjustment cylinders from an initial force level to a maximum test force. The stiffness matrices have been slightly tuned to account for modeling errors. As shown in Fig. 3, the error

$e_{y,k} = \Delta y_{\text{im,meas},k} - \Delta y_{\text{im,calc},k}$ between the calculated and the measured roll intermesh is lower than 0.1 mm for all measured points. These error values are lower than the adjustment accuracy of the actuators of the leveler.

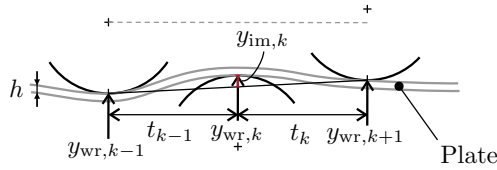


Fig. 2. Definition of work roll intermesh.

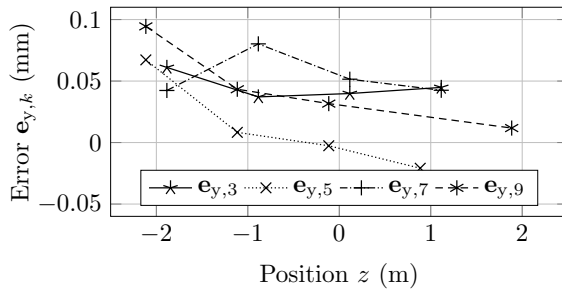


Fig. 3. Error between measured and calculated roll intermesh.

3. PLATE MODEL

In this section, a plate model is presented. Its main purpose is to calculate the distributed forces $q_k(z)$ exerted on the work rolls due to the leveling deformation of the plate. To simplify the calculation, the plate is divided into several independent stripes, which can be modeled as beams. The force-deflection relations are then individually solved for each stripe.

The basic principle of the leveling process is to eliminate the unknown initial residual stress state by excessive plastic deformation during the first few bends and to impose a desired stress distribution by decreasing alternate plastic deformation during the subsequent bending steps. This explains why both the sequential stress distributions and the leveling forces depend on the (plastic) bending history of the plate. Thus, a model which adequately captures this effect is required.

3.1 The leveling model by Henrich

The leveling model by (Henrich, 1993) was developed as a tool to determine optimal leveler adjustments. The model is individually evaluated for each stripe j and its main results are the corresponding (concentrated) leveling forces $\mathbf{F}_{s,j} = [F_{j,k}]$ on the rolls for a given roller configuration $(\mathbf{x}_j, \mathbf{y}_j)$. Here $\mathbf{x}_j = [x_{j,k}]$ and $\mathbf{y}_j = [y_{j,k}]$ denote the absolute positions of all work roll axes at the point z_j of the respective stripe j . Henrich's model provides a good insight into the leveling process because it also gives the strain distribution $\varepsilon_k(y)$ and the stress distribution $\sigma_k(y)$ at each bending step k . The model iteratively solves the static beam equation of an elasto-plastically deformed

Euler-Bernoulli beam. The nonlinear material behavior of the plate is approximated by a linear-elastic linear-plastic stress-strain relation, which can also incorporate some typical work hardening mechanisms.

Based on the static equilibrium of moments, it is clear that the bending moment M of a beam only loaded with shear forces has a piecewise linear shape along the direction x as shown in Fig. 4. This must also hold for plastic deformation. Henrich's solution algorithm (c.f. Fig. 5) uses a piecewise polynomial ansatz (spline) for the elastic-plastic deflection curve of a beam, as indicated in the top part of Fig. 4. The algorithm iteratively adapts the boundary points $x_{A,k}$ (roll contact points) and $x_{G,k}$ (transition from purely elastic bending to elasto-plastic bending) to achieve a piecewise linear moment characteristics. Note that the contact points $x_{A,k}$ do not necessarily coincide with the vertex points $x_{j,k}$ of the work rolls. In each iteration, the stress distributions $\sigma_k(y)$ and the bending moments $M_k = M(x_{A,k})$ are calculated for all bending steps k .

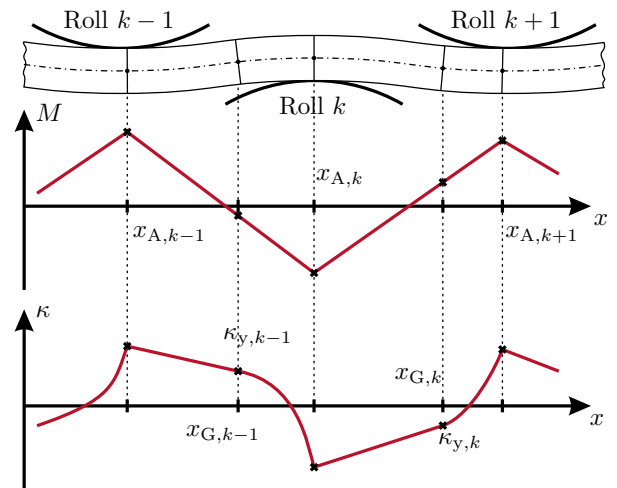


Fig. 4. Shape of the deformed plate, bending moment M , and curvature κ .

Henrich's leveling model has been extensively studied in the literature and generally yields accurate results (c.f. Doege et al. (2002); Dratz et al. (2009)). The main benefit of the model is its simplicity while covering all important aspects of the leveling process. However, the calculation of the full stress profiles $\sigma_k(y)$ is computationally expensive and in fact not always necessary.

3.2 A tailored leveling model

Henrich's solution algorithm offers a wide range of adjustable parameters to analyze the leveling process. However, to calculate a sufficiently accurate approximation of the leveling forces, only a reduced set of parameters is required. Moreover, a typical leveling process allows the following assumptions, which simplify the solution process, c.f. (Batty and Lawson, 1965).

First, a linear-elastic ideal-plastic stress-strain relation of the material, as shown in Fig. 6 (a), is assumed. Second,

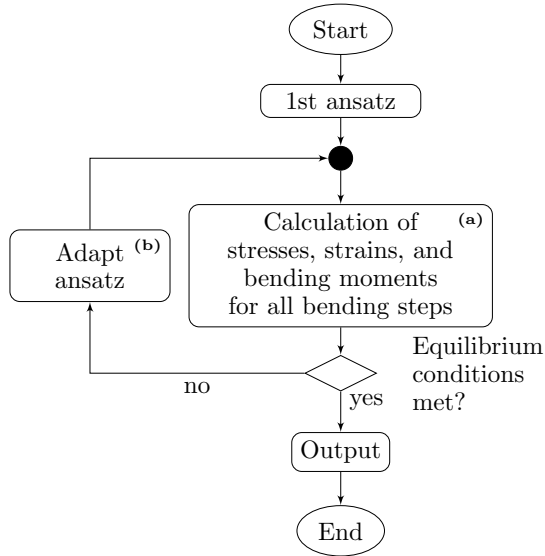


Fig. 5. Flowchart of Henrich's solution algorithm.

it is assumed that the initial residual curvature is small, i.e., $\kappa_1 = \kappa_{\text{res}} \approx 0$ and that the initial residual stress distribution vanishes, i.e., $\sigma_{\text{res}}(y) = 0$. A third assumption is that the curvatures κ_k at the consecutive bending steps k satisfy the following inequality relations

$$|\kappa_2| > 0 \quad (7a)$$

$$|\kappa_3| > |\kappa_2| \quad (7b)$$

$$|\kappa_{k+1}| \leq |\kappa_k| \quad \text{for } k \geq 3. \quad (7c)$$

That is, the curvature rapidly increases until step $k = 3$, which eliminates (unknown) initial residual stresses. For the considered leveler, the maximum curvature is usually achieved at the 3rd roll. In the subsequent steps, the curvature is decreased to establish the desired stress distribution. Under the assumptions above, it is possible to directly calculate the bending moment for given curvatures as indicated in Fig 6 (b).

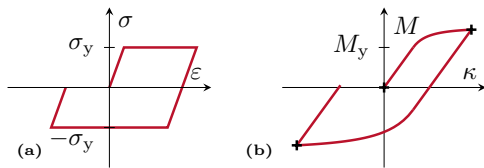


Fig. 6. Linear-elastic ideal plastic stress-strain relations (a) and corresponding curvature-moment relations (b).

The bending moment of a beam with the height (plate thickness) h and the width b_j

$$M_k = -2b_j \int_0^{\frac{h}{2}} y \sigma_k(y) dy \quad (8)$$

can be evaluated if the stress distribution $\sigma_k(y)$ over the cross section of the beam is known. The previous assumptions lead to two different cases for the calculation of the bending moment in the elastic-plastic region: In case one, if the residual stress is completely overwritten (i.e., the maximum curvature is large enough), the elastic-

plastic bending moment is independent of the previous steps and can be written as

$$M_k = \text{sgn}(\kappa_k) \left(3 - \frac{\kappa_y^2}{\kappa_k^2} \right) \frac{S}{2} \sigma_y \quad (9)$$

with the yield curvature $\kappa_y = \frac{2\sigma_y}{Eh}$ (onset of plastic deformation), the Young's modulus E , the elastic section modulus $S = \frac{b_j h^2}{6}$, and the yield strength σ_y of the plate material. In the second case, the absolute curvature values monotonically decrease from a (known) maximum value. Then the bending moment M_{k+1} can be expressed in terms of the change of curvature $\Delta\kappa_k = \kappa_{A,k+1} - \kappa_{A,k}$, $\Delta\kappa_{y,k} = \kappa_{y,k} - \kappa_{A,k}$ and the previous bending moment M_k . If the deformation is purely elastic, i.e., $|\Delta\kappa_k| \leq |\Delta\kappa_{y,k}|$,

$$M_{k+1} = M_k + EI \Delta\kappa_k, \quad (10)$$

otherwise (elasto-plastic bending)

$$M_{k+1} = M_k + \text{sgn}(\Delta\kappa_k) \left(3 - \frac{\Delta\kappa_{y,k}^2}{\Delta\kappa_k^2} \right) S \sigma_y. \quad (11)$$

In (10), $I = \frac{b_j h^3}{12}$ is the 2nd moment of area of the beam cross section.

Equations (9)–(11) facilitate a direct calculation of all required values of the consecutive bending process as outlined in Fig. 7. These equations replace part (a) of

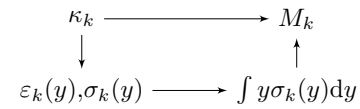


Fig. 7. Algorithm (a).

Henrich's algorithm in Fig. 5 and significantly reduce the overall computational load of the algorithm. The computation time with MATLAB® R2016a on a 3.4 GHz CPU is reduced from about 0.8s for Henrich's original algorithm to 0.16s for the improved algorithm if maximum 50 iterations are used. To achieve accurate results for the leveling forces, only 5 to 10 iterations are usually required.

To assemble the model for the whole plate, consider that the plate is approximated by m independent stripes with the width b_j . Let

$$\mathbf{F}_{s,j} = [F_{j,1}, \dots, F_{j,k}, \dots, F_{j,11}]^T = g(\mathbf{y}_j) \quad (12)$$

be a short notation of the leveling forces of a single stripe j calculated by the proposed algorithm. Then the full model of the whole plate can be assembled in the form

$$\mathbf{F}_s = [\mathbf{F}_{s,1}^T, \dots, \mathbf{F}_{s,j}^T, \dots, \mathbf{F}_{s,m}^T]^T = \mathbf{g}(\mathbf{y}_s) \quad (13)$$

with $\mathbf{y}_s = [\mathbf{y}_j]$ where $j = 1, \dots, m$.

4. DEFLECTION MODEL

4.1 Combination of machine and plate model

To finalize the mathematical deflection model, the machine and the plate model are combined in this section. Although the leveling forces are distributed forces along the direction z , the strip model gives concentrated forces $\mathbf{F}_{s,j}$ for each stripe, cf. (13). It is assumed that the leveling force is

uniform along the direction z within each stripe, i.e., the distributed total leveling force $q_k(z)$ of a work roll k has a piecewise constant shape with the values $\frac{F_{j,k}}{b_j}$, $j = 1, \dots, m$. The nodes of the machine do not necessarily coincide with those of the plate model. Based on the finite element method, the nodal forces on a work roll k are obtained by evaluating the integrals

$$f_{k,i,p} = \int_{z_{wr,i}}^{z_{wr,i+1}} q_k(z) \varphi_p(z) dz \quad (14)$$

with the distributed load $q_k(z)$ and the test functions $\varphi_p(z)$, $p = 1, \dots, 4$ for each element $i = 1, \dots, n$. The Euler-Bernoulli beam-element has two degrees of freedom at each node, the test functions are Hermite polynomials. By assembling of (14) for all elements i , the linear relation $\mathbf{F}_{wr} = \mathbf{A}^T \mathbf{F}_s$ between the stripe forces \mathbf{F}_s and the nodal work roll forces \mathbf{F}_{wr} is obtained. According to the virtual work principle, the relation $\mathbf{y}_s = \mathbf{A} \mathbf{y}_{wr}$ must hold for the vertical displacements of the stripes and work rolls. The deflection problem can then be obtained by combining (6) and (13) in the form

$$\mathbf{R}(\mathbf{y}_{wr}) = \mathbf{y}_{wr} - \mathbf{f}(\mathbf{ad}, \mathbf{A}^T \mathbf{g}(\mathbf{A} \mathbf{y}_{wr})) = \mathbf{0}. \quad (15)$$

This relation can be numerically solved for the displacements \mathbf{y}_{wr} of the work rolls by means of the Levenberg-Marquardt algorithm. This method requires the Jacobian

$$\mathbf{J} = \frac{d\mathbf{R}}{d\mathbf{y}_{wr}} = \mathbf{I} - \underbrace{\frac{d\mathbf{f}}{d\mathbf{F}_{wr}}}_{\mathbf{J}_F} \mathbf{A}^T \underbrace{\frac{d\mathbf{g}}{d\mathbf{y}_s}}_{\mathbf{J}_s} \mathbf{A}. \quad (16)$$

The Jacobian of the machine model

$$\mathbf{J}_F = \frac{d\mathbf{f}}{d\mathbf{F}_{wr}} = \left(\tilde{\mathbf{K}}_{frm} + \mathbf{K}_{wr} \right)^{-1} \quad (17)$$

is the flexibility matrix of the leveler. The Jacobian of the plate model \mathbf{J}_s is numerically determined using finite differences. The nonlinearity of the problem (15) is moderate, which implies that \mathbf{J} does not change significantly during the iterative solution process. In fact, rapid convergence is even achieved if \mathbf{J} is computed only during the first iteration and if the same values are used in all subsequent iterations.

4.2 Model validation

To verify the combined model, several load cases that occurred during the production process of the considered plate leveler are studied. The forces in the adjustment cylinders were measured for different leveling passes. Because the plates were laterally centered and symmetric, the mean values of the forces on the entry and exit side cylinders are used for validation. The leveling force on each work roll cannot be measured. However, the difference between the forces on the entry and the exit side of the leveler provide a good indication of the force distribution within the leveler.

Table 1 contains the measured and the calculated mean adjustment cylinder forces for three load cases. The first two rows show force values for two passes of a plate with the width $b = 2.5$ m, the thickness $h = 15.1$ mm, and the yield strength $\sigma_y = 424$ MPa. In the first case, the set points were chosen for the nominal yield strength $\sigma_y = 424$ MPa. In the second case, the set points were chosen as if the leveler would process a plate with a yield strength

of $\sigma_y = 550$ MPa. This leads to a higher plastification rate and higher leveling forces. In the third row, force values for a plate with the same yield strength and thickness but a width of $b = 3.0$ m are shown.

The distribution of the forces between entry and exit side is adequately captured by the model. The calculated absolute force values differ roughly 10% from the measured forces. This is to be expected because the actual yield strength of the plate can easily vary within a range of $\pm 10\%$. Note that the plate model is calculated with nominal parameters only.

Table 1. Comparison of adjustment cylinder forces (kN) for different plates with thickness $h = 15.1$ mm and yield strength $\sigma_y = 424$ MPa.

	$\bar{F}_{en,meas}$	$\bar{F}_{en,calc}$	$\bar{F}_{ex,meas}$	$\bar{F}_{ex,calc}$
$b = 2.5$ m	1835	1954	716	869
$b = 2.5$ m	2074	2105	931	1189
$b = 3.0$ m	2377	2105	1048	1188

5. OPTIMAL LEVELER ADJUSTMENT

In the last part of this paper, the developed model is used to calculate optimal adjustment set points. Based on the model, the limits of the load and the adjustment values can be systematically considered in a constrained optimization problem. A successful leveling process highly depends on the consecutive curvature values imposed on the plate. Therefore, the degrees of freedom of the leveler have to be utilized to set certain roll gap values which guarantee that the plate undergoes a bending process with the desired curvature values.

Based on the leveling theory, nominal adjustment values $y_{d,k}$ for the upper work rolls can be determined. These values lead to a reference curvature $\kappa_{d,k}$ for each bending step k . Due to the elastic deformation of the leveler, the actual positions of the work rolls differ from the nominal reference positions and, therefore, the curvature. In order to compensate the deflection of the machine, additional adjustment values \mathbf{ad}_{comp} have to be determined. This gives the new reference adjustment

$$\mathbf{ad}_{ref} = \mathbf{ad}_{cal} + \mathbf{ad}_{nom} + \mathbf{ad}_{comp}. \quad (18)$$

The adjustment \mathbf{ad}_{cal} is determined when calibrating the leveler. During the calibration process, the adjustment for a given test load is measured. All future adjustments are relative to the calibrated adjustment. An exact compensation of the deflection of the machine is impossible due to the finite number and the bounds of the adjustment variables. This is why a constrained optimization problem is formulated to find optimal values \mathbf{ad}_{comp} .

5.1 Optimal deflection compensation

The constrained static optimization problem is chosen in the form

$$\mathbf{ad}_{opt,comp} = \arg \min_{\mathbf{ad}} \sum_{j=1}^m \sum_{k=1}^{11} \gamma_{k,j} (\kappa_{d,k} - \kappa_{k,j})^2 \quad (19a)$$

$$\text{s.t. } \mathbf{R}(\mathbf{y}_{wr}) = 0$$

$$\mathbf{ad}_{min} \leq \mathbf{ad} \leq \mathbf{ad}_{max} \quad (19b)$$

$$F_{sr,k,i} < F_{sr,max}. \quad (19c)$$

This problem minimizes the quadratic error between the desired and the actual curvature values of each stripe j and each work roll k . The user-defined weighting parameters $\gamma_{k,j} > 0$ provide means to emphasize specific bending steps or stripes.

To account for force and adjustment limits the constraints (19b) and (19c) have to be considered. The constraint (19c) ensures that support rolls are not overloaded, which could entail breakage of the rolls or their bearings. If constraints are active, it may happen that the desired plastification of the plate is not reached. The optimization problem (19) can be solved, for example, by an active-set method or an interior-point algorithm. In this paper, (19) is solved by the interior-point algorithm provided by MATLAB®.

5.2 Numerical results

To show the feasibility of the optimization approach, an example of a plate with the yield strength $\sigma_y = 425$ MPa, the width $b = 2.5$ m, and the thickness $h = 10$ mm is considered. The plate is divided into 5 stripes. In this example, only the parallel adjustment of the traverse ad_m and the symmetric adjustment of the bending frame $ad_{bf,drs} = ad_{bf,ops} = ad_{bf}$ are used as optimization variables.

In Fig. 8, the nominal and the actual curvature values of the first three stripes are shown (the plate is symmetric). The upper diagram shows the curvature values for the nominal adjustment without compensation. It is obvious that the calibration adjustment ad_{cal} overcompensates the deflection for the considered plate. In the lower diagram, the actual curvature values are in good accordance with the reference values for each stripe. The optimization algorithm adjusts the bending frame properly in order to compensate the deflection of the machine and also reduces the parallel adjustment ad_m to account for the undesired overcompensation caused by ad_{cal} .

REFERENCES

- Batty, F. and Lawson, K. (1965). Heavy plate levellers. *Journal of The Iron and Steel Institute*, 203, 1115–1128.
- Baumgart, M., Steinboeck, A., Kugi, A., Douanne, B., Raffin-Peyloz, G., Irastorza, L., and Kiefer, T. (2011). Modeling and active compensation of the compliance of a hot leveler. *Steel Research International*, Special Edition: 10th International Conference on Technology of Plasticity, ICTP 2011, 337–342.
- Baumgart, M., Steinboeck, A., Kugi, A., and Kiefer, T. (2015). Modeling and experimental validation of the deflection of a leveller for hot heavy plates. *Mathematical and Computer Modelling of Dynamical Systems*, 21(3), 202–227.
- Baumgart, M., Steinboeck, A., Kugi, A., Raffin-Peyloz, G., Irastorza, L., and Kiefer, T. (2012). Optimal active deflection compensation of a hot leveler. In *Preprints of the IFAC Workshop on Automation in the Mining, Mineral and Metal Industries*, 30–35. Gifu, Japan.
- Bodini, L., Ehrich, O., and Krauhausen, M. (2007). Heavy plate leveler improvement by coupling a model to a flatness gauge. In *Proceedings of the 3rd International Steel Conference on New Developments in Metallurgical*

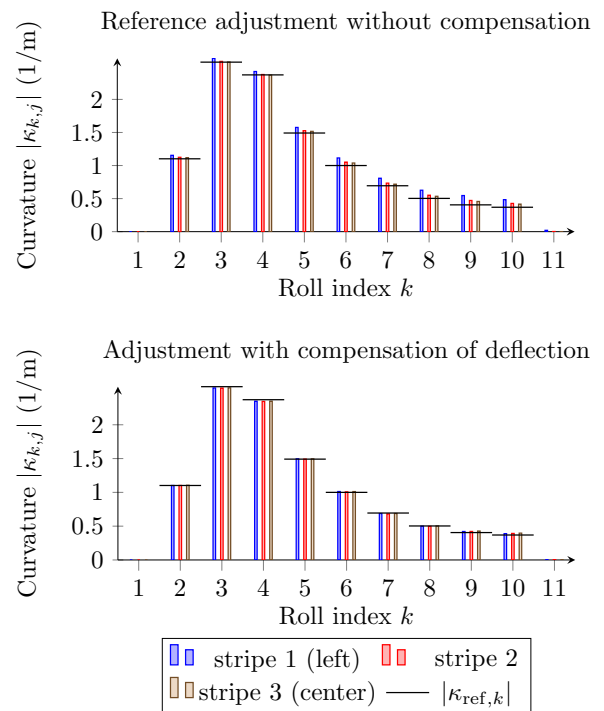


Fig. 8. Simulated curvature of stripes with nominal and optimized adjustment.

- Process Technologies*, 246–251. Steel Institute VDEh, Düsseldorf, Germany.
- Doerge, E., Menz, R., and Huinink, S. (2002). Analysis of the levelling process based upon an analytic forming model. *CIRP Annals - Manufacturing Technology*, 51(1), 191–194.
- Dratz, B., Nalewajk, V., Bikard, J., and Chastel, Y. (2009). Testing and modelling the behaviour of steel sheets for roll levelling applications. *International Journal of Material Forming*, 2(1), 519–522.
- Henrich, L.S. (1993). *Theoretische und experimentelle Untersuchungen zum Richtwalzen von Blechen*. Ph.D. thesis, Fachbereich Maschinentechnik, Universität-Gesamthochschule Siegen, Germany.
- Krämer, S., Dehmel, R., Horn, G., Koch, T., Lemke, J., and Lixfeld, P. (2011). Plate production using most modern process models. In *4th International Conference on Modelling and Simulation of Metallurgical Processes in Steelmaking, STEELSIM, METEC InSteelCon 2011*. Düsseldorf, Germany.
- Liu, Z., Wang, Y., and Yan, X. (2012). A new model for the plate leveling process based on curvature integration method. *International Journal of Mechanical Sciences*, 54(1), 213–224.
- Menz, R. (2002). *Entwicklung eines analytischen Simulationsmodells als Grundlage einer geregelten Richtmaschine*, volume 601 of *Verein Deutscher Ingenieure: Fortschrittberichte VDI, Berichte aus dem Institut für Umformtechnik und Umformmaschinen*, Universität Hannover. VDI-Verlag, Hannover.
- Mischke, J. and Jonca, J. (1992). Simulation of the roller straightening process. *Journal of Materials Processing Technology*, 34(14), 265–272.